

Detection of an orbital period in the supergiant high mass X-ray binary IGR J16465–4507 with *Swift*-BAT

V. La Parola¹, G. Cusumano¹, P. Romano¹, A. Segreto¹, S. Vercellone¹, G. Chincarini^{2,3}

¹INAF, Istituto di Astrofisica Spaziale e Fisica Cosmica, Via U. La Malfa 153, I-90146 Palermo, Italy

²INAF-Osservatorio Astronomico di Brera, I-23807 Merate (LC), Italy

³Università degli Studi di Milano, Bicocca, I-20126 Milano, Italy

ABSTRACT

We analysed the IGR J16465–4507 Burst Alert Telescope survey data collected during the first 54 months of the *Swift* mission. The source is in a crowded field and it is revealed through an ad hoc imaging analysis at a significance level of ~ 14 standard deviations. The 15–50 keV average flux is $\sim 3 \times 10^{-11}$ erg cm $^{-2}$ s $^{-1}$. The timing analysis reveals an orbital period of 30.243 ± 0.035 days. The folded light curve shows the presence of a wide phase interval of minimum intensity, lasting $\sim 20\%$ of the orbital period. This could be explained with a full eclipse of the compact object in an extremely eccentric orbit or with the passage of the compact source through a lower density wind at the orbit apastron. The modest dynamical range observed during the BAT monitoring suggests that IGR J16465–4507 is a wind-fed system, continuously accreting from a rather homogeneous wind, and not a member of the Supergiant Fast X-ray Transient class.

Key words: X-rays: binaries – X-rays: individual: IGR J16465–4507.
Facility: *Swift*

1 INTRODUCTION

High mass X-ray binaries (HMXBs), stellar systems composed of a compact object and an early-type massive star, are traditionally divided in two subclasses (e.g. van Paradijs 1995, and references therein), depending on the nature of the high mass primary and, consequently, the different mass-transfer and accretion mechanism. On one side are the systems with main sequence Be primaries (Be-HMXBs). They are generally wide ($P_{\text{orb}} \gtrsim 10$ d) eccentric (eccentricity $e \sim 0.3\text{--}0.5$) systems in which the primaries are not filling their Roche lobe, and accretion onto the compact object occurs from the equatorial region of the rapidly rotating Be star. Most of these systems are highly variable: in some of them recurrent outbursts are observed caused by an enhanced rate when the compact star passes close to the Be star. On the other side are the systems with an evolved OB supergiant primary (sgHMXB). Their periods are shorter ($P_{\text{orb}} \lesssim 10$ d) and their orbits more circular than in Be-HMXBs. They are powered either by a geometrically thin accretion disc or by the strong radiation-driven stellar wind, depending on whether the primary fills its Roche lobe or not. Their X-ray emission is bright and persistent.

Recently, this rather clear-cut picture was made more structured with the INTEGRAL observations of the Galactic plane. Two additional classes were added to the classical OB primary HMXBs: the highly absorbed persistent systems (Walter et al. 2004, 2006) and the supergiant fast X-ray transients (SFXTs, Sguera et al. 2005; Negueruela et al. 2006; Smith 2004; in't Zand 2005). The

former are characterized by orbital and spin periods consistent with those observed in wind-accreting systems, but a much higher absorbing column density. The latter are transient sources showing a large dynamic range of 3–5 orders of magnitude with sporadic outbursts (which however are significantly shorter than those of typical Be-HMXBs), characterized by bright flares lasting up to days with peak luminosities of $10^{36}\text{--}10^{37}$ erg s $^{-1}$ (Sguera et al. 2005; Romano et al. 2009; Sidoli et al. 2009).

The Burst Alert Telescope (BAT, Barthelmy et al. 2005) on board *Swift* (Gehrels et al. 2004) is performing a continuous coverage of the hard X-ray sky (50 to 80% of the sky every day). This allowed the detection of many of the new INTEGRAL HMXBs (e.g. Cusumano et al. 2009) and the collection of their long term light curves. In this Letter we analyse the hard X-ray data collected during the first 54 months of *Swift*-BAT sky monitoring using data in the region of the IGR J16465–4507. This source was discovered by INTEGRAL in 2004 (Lutovinov et al. 2004) and X-ray activity was observed with IBIS/ISGRI starting on September 6, at a flux level of 8.8 ± 0.9 mCrab (18–60 keV), followed by a flare (up to 28 mCrab) on September 7. Follow-up observations with XMM-Newton revealed pulsations at 228 ± 6 s (Lutovinov et al. 2005) and allowed the identification of the optical counterpart with 2MASS J16463526–4507045 (Zurita Heras & Walter 2004). This was classified as a B0.5 Ib supergiant at a distance of ~ 8 kpc (Negueruela et al. 2007) or as a O9.5 Ia supergiant at a distance of $9.5^{+14.1}_{-5.7}$ kpc (Nespoli et al. 2008). The supergiant nature of the companion, combined with the

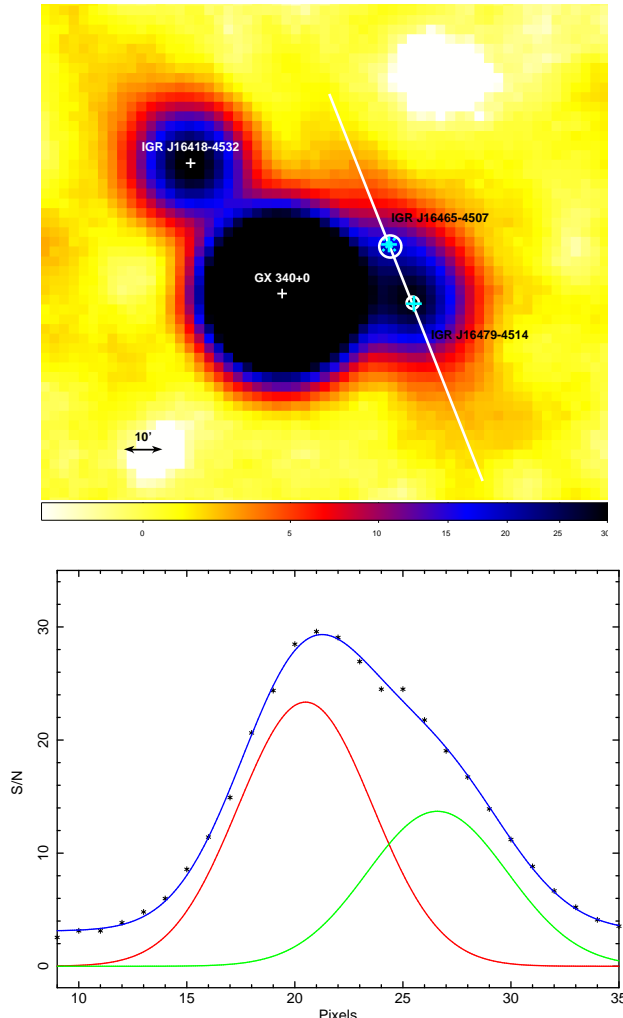


Figure 1. Top: 15–50 keV significance map in the neighborhood of IGR J16465–4507. The color-bar represents the significance levels. The cyan star marks the XMM position (Zurita Heras & Walter 2004) of IGR J16465–4507. The white circles are centered on the position derived by fitting the significance profile extracted along the white line with two Gaussians plus a constant; their radius corresponds to the 90% error on the position. **Bottom:** Significance profile extracted along the white line in the above map. The plot shows the data (stars) and the best fit model (blue line, the sum of two Gaussian profiles plus a constant value). The higher peak (red line) corresponds to IGR J16479–4514, the lower peak (green line) corresponds to IGR J16465–4507.

observed hard X-ray variability (Lutovinov et al. 2004) and the X-ray spectral distribution, modeled by a hard power law with photon index 1.0 ± 0.52 (Lutovinov et al. 2005), suggested a classification of this source as a SFXT (Negueruela et al. 2006). However, Walter & Zurita Heras (2007), based on INTEGRAL measurements, suggested that IGR J16465–4507 is likely a classical supergiant HMXB, with an average flux just below the IBIS/ISGRI sensitivity undergoing sporadic long periods of enhanced activity.

This Letter is organized as follows. Section 2 describes the BAT data reduction and the imaging analysis. Section 3 reports on the timing analysis. Sect. 4 describes the analysis of the pointed soft X-ray observation with *Swift*-XRT. In Sect. 5 we briefly discuss our results. Errors are at 90 % confidence level, if not stated otherwise.

2 IMAGING ANALYSIS

We analysed the BAT survey data of the first 54 months of the *Swift* mission. We retrieved the raw data from the HEASARC public archive¹ and processed them with a dedicated software (Segreto et al. 2010) that performs screening, mosaicking and source detection on data from coded mask instruments. The code also produces light curves for any given sky position.

Figure 1 (top panel) shows the 15–50 keV significance sky map (exposure time of 17.7 Ms) in the direction of the sgHMXB IGR J16465–4507. The position of the source (Zurita Heras & Walter 2004) is marked with a cyan cross. The source is in a crowded field, at 16.8 arcmin from the SFXT IGR J16479–4514 and 30.8 arcmin from the low mass X-ray binary GX340+0 and for this reason it is not detected with our code. However, the significance profile extracted along the line crossing the position of IGR J16479–4514 and IGR J16465–4507 shows an asymmetric shape that can not be fitted with a constant plus a single Gaussian (the root mean square deviation is 48.8) and suggests the contribution of more than one source. The profile is instead well fitted with a constant plus a double Gaussian (the root mean square deviation is 3.2 and the data points are uniformly distributed around the model) peaking at the position of the two sources, with the weaker source (IGR J16465–4507) at the significance of 13.7 standard deviations (Fig. 1, bottom panel).

Moreover, the presence of IGR J16465–4507 is confirmed by the analysis of the sky map produced using data selected in time intervals when the nearby source IGR J16479–4514 was in eclipse (Bozzo et al. 2008; Jain et al. 2009). In this map (3.4 Ms exposure) IGR J16465–4507 is detected with a signal-to-noise $S/N \sim 8$.

3 TIMING ANALYSIS

We extracted the light curve of IGR J16465–4507 in the 15–50 keV energy range with the maximum time resolution allowed by the data (~ 300 s), subtracting the contamination of the nearby sources as detailed in Segreto et al. (2010). The photon arrival times were corrected to the Solar system barycenter (SSB) by using the task EARTH2SUN.

We looked for evidence of orbital periodicities in the BAT data. A folding technique was applied to the baricentred arrival times by searching in the 0.5–100 d period range with a step resolution of $P^2/(N \Delta T)$, where $N = 16$ is the number of phase bins and ΔT (140,213,559.0 s) is the data time span. The average rate in each phase bin was evaluated by weighting the light curve rates by the inverse square of the corresponding statistical error:

$$R_j = \frac{\sum r_i / er_i^2}{\sum 1 / er_i^2} \quad (1)$$

where R_j is the average rate in the j -th phase bin ($j=1,16$) of the trial profile, r_i are the rates of the light curve whose phase fall into the j -th phase bin and er_i are the corresponding statistical errors. The error on R_j is $(\sqrt{\sum 1 / er_i^2})^{-1}$. This procedure, adopted to deal with the large span in er_i , is justified by the fact that the data are background dominated. Figure 2 (a) shows the resulting periodogram. We find significant evidence for periodicity ($\chi^2 \sim 251.8$) at a period of $P_{\text{orb}} = 30.243 \pm 0.035$ days (the two features at higher periods are multiple of P_{orb}) where the error is the period resolution. We observe that the average χ^2 in the periodogram is far from the

¹ <http://heasarc.gsfc.nasa.gov/cgi-bin/W3Browse/w3browse.pl>

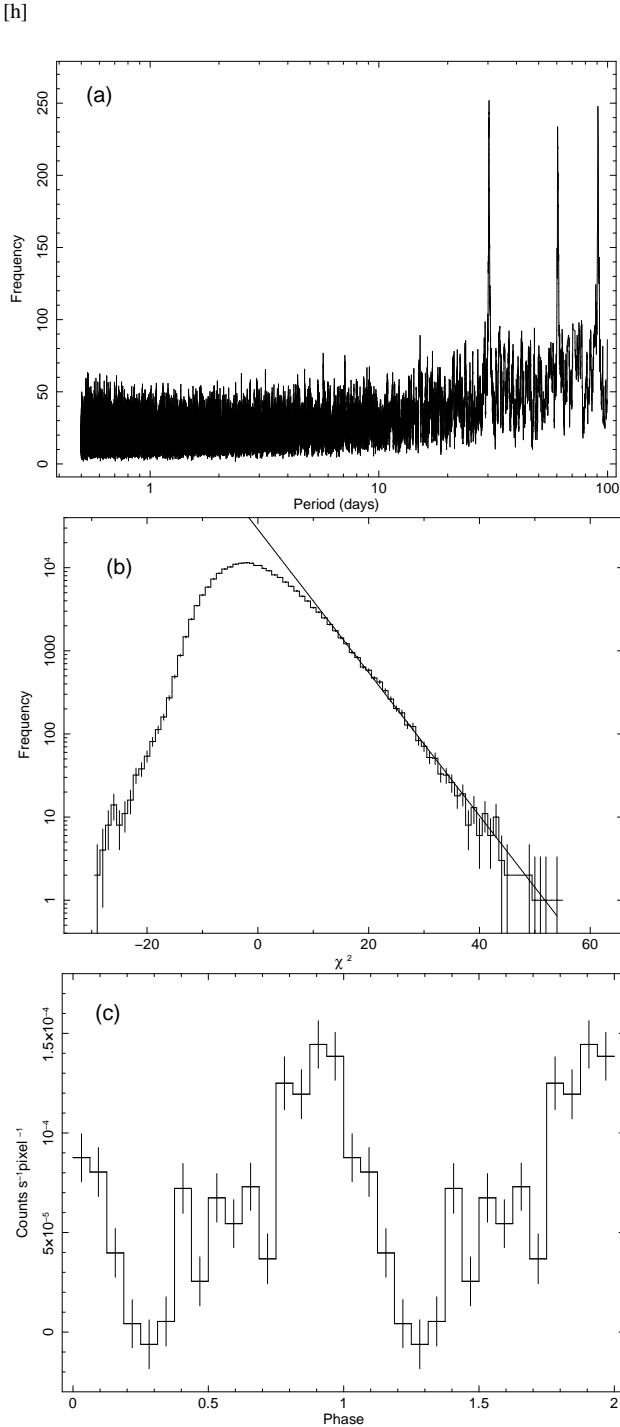


Figure 2. (a): Periodogram of *Swift*-BAT (15–50 keV) data for IGR J16465-4507. (b): Distribution of χ^2 values extracted around P_{orb} , in the period range between 0.5 and 40 days excluding the values between 29.243 and 31.243 days. The continuous line is the best fit obtained with an exponential model applied to the tail of the distribution ($\chi^2 > 15$). (c): *Swift*-BAT Light curve folded at a period $P = 30.243$ day, with 16 phase bins.

average value expected for white noise ($N - 1$) and increases with increasing trial periods. As a consequence, the χ^2 statistics cannot be applied to evaluate the significance of the detected periodicity. In order to have an estimate of the significance of the observed feature we performed the following steps:

(1) we corrected the χ^2 distribution by subtracting the trend modeled with a 2nd order polynomial fit. The value at P_{orb} subtracted for the pedestal is 206.7.

(2) we computed the histogram of the resulting χ^2 distribution between 0.5 and 40 days [Figure 2 (b)], excluding the peak region (29.243–31.243 days).

(3) we fit the distribution for $\chi^2 > 15$ with an exponential function and evaluated the integral of the best-fit function beyond 206.7. This integral yields a number of chance occurrences due to noise of 2.03×10^{-13} corresponding to a significance of the detected temporal feature of ~ 7.3 standard deviations in Gaussian statistics.

As an alternative method to evaluate the significance of the temporal feature we produced 2000 light curves performing a random distribution of the observed rates in the bin times of the original light curve. A periodogram between 0.5 and 100 days [51673.0 trial periods with the resolution of $P^2/(N \Delta T)$] was calculated for each of them obtaining a maximum χ^2 value of 91.5 in the whole sample. This corresponds to a significance of the observed periodicity higher than 5.5 standard deviations.

In order to exclude the presence of systematic features in the periodogram, we performed the same analysis on the light curve of the two nearby sources (IGR J16479-4514 and GX 340+0). We found no evidence for any significant feature at P_{orb} .

In Fig. 2 (c) we show the pulsed profile folded at P_{orb} with $T_{\text{epoch}} = 54172.4236$ MJD. There is clear evidence for a phase consistent with null intensity, whose centroid, evaluated by fitting the data around the dip with a Gaussian function, is at phase 0.268 ± 0.015 , corresponding to $\text{MJD} (54180.5 \pm 0.5) \pm n P_{\text{orb}}$.

The BAT light curve at the time resolution of 1 day (Fig. 3) (top panel) shows no evidence for the presence of flare episodes throughout the period of monitoring. The average count rate is $(6.9 \pm 0.5) \times 10^{-5}$ counts s^{-1} pixel $^{-1}$ and the maximum count rate spread is consistent within 3 standard deviations with the average. Figure 3 (bottom panel) shows the 54-months BAT light curve with a bin time of P_{orb} , excluding bins with an exposure fraction less than 5%. The source is detected in most of the time bins (30 out of 38). Adopting the best fit model of the INTEGRAL data (Lutovinov et al. 2005), the average count rate corresponds to an observed 15–50 keV flux of 2.36×10^{-11} erg cm^{-2} s^{-1} (2.3 mCrab). Assuming a distance of 9.5 kpc (Nespoli et al. 2008), the average luminosity is 2.6×10^{35} erg s^{-1} .

4 SOFT X-RAY DATA

The source was observed by *Swift*-XRT on 2009 June 13 (ObsId 00037885001, 2.3 ks net exposure). The epoch of the observation corresponds to an orbital phase of ~ 0.2 . The data were processed with standard techniques with the FTOOLS in the HEASOFT package (v.6.8). Figure 4 shows the background subtracted 0.3–10 keV light curve, with a time bin of 300 s.

The statistic content of the XRT data is too low for a meaningful spectral analysis. In order to convert the observed count rate into 0.3–10 keV flux we have used the best fit model obtained by Lutovinov et al. (2005) for the XMM data. We obtain an observed flux in the 0.3–10 keV energy band of 1.16×10^{-11} erg cm^{-2} s^{-1} .

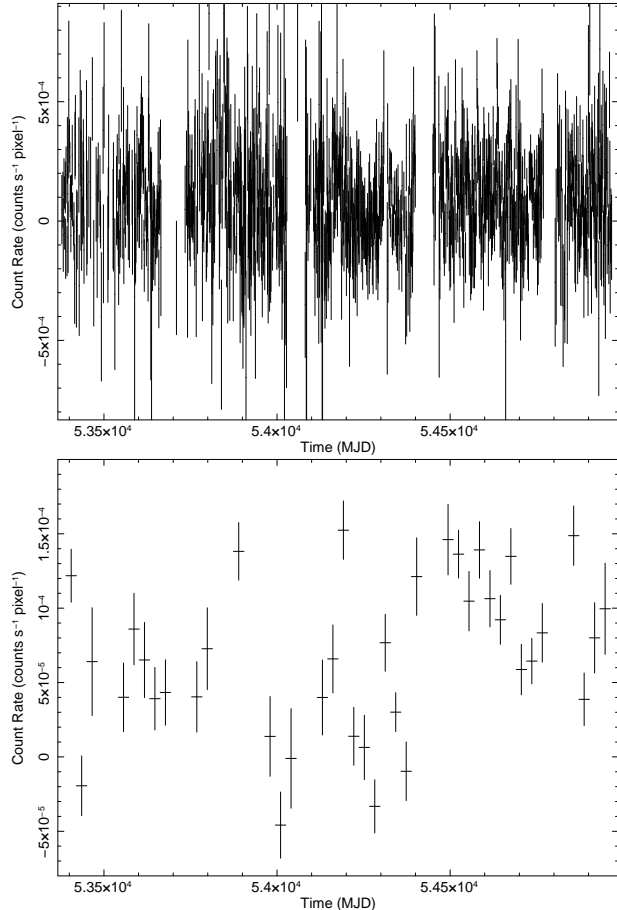


Figure 3. **Top panel:** BAT light curve with a bin time of 1 day . **Bottom panel:** BAT light curve with a bin time of P_{orb} .

This corresponds to an X-ray luminosity $L_X \sim 1.2 \times 10^{35}$ erg s⁻¹ in the same band.

5 DISCUSSION AND CONCLUSIONS

We have analysed the data collected by *Swift*-BAT during the first 54 months of the *Swift* mission in the region of the supergiant HMXB IGR J16465–4507. The source is detected at a significance level of ~ 14 standard deviations with an average flux of $\sim 2.36 \times 10^{-11}$ erg cm⁻² s⁻¹ in the 15–50 keV energy band.

The light curve reveals a periodicity of 30.243 ± 0.035 days that we interpret as the orbital period of the binary system.

By applying Kepler's third law, the semi-major axis of the binary system is given by $a^3 = P_{\text{orb}}^2 \times G(M_\star + M_X)/4\pi^2$, where M_\star and M_X are the masses of the supergiant and compact object, respectively. We adopt $M_X = 1.4 M_\odot$ and $M_\star = 27.8 M_\odot$ (Martins et al. 2005, for an O9.5 I star of radius $R_\star = 22.1 R_\odot$). This yields $a \sim 125 R_\odot \sim 6 R_\star$. We note that the assumption of a stellar type B0.5 Ib would lead to an estimate of $a \sim 150 R_\odot \sim 5 R_\star$ (Searle et al. 2008, $M_\star = 47 M_\odot$, $R_\star = 32.2 R_\odot$).

The folded profile shows the presence of a dip with a count rate consistent with no emission, that could be interpreted as a full eclipse. However, the width of this dip ($\sim 20\%$ of P_{orb}) is not consistent with the duration of the eclipse expected for a circular orbit with $6 R_\star$ semimajor axis, assuming an edge-on inclination. To ob-

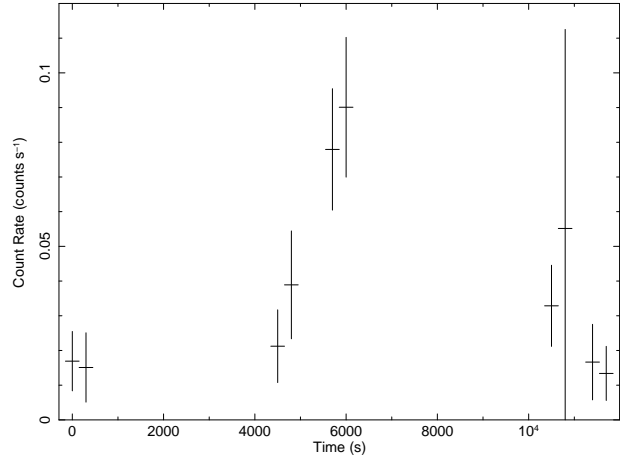


Figure 4. XRT light curve binned at 300 s.

tain such a long eclipse, the system should have an eccentricity of at least 0.8 coupled with a high inclination. This scenario is unlikely. Alternatively, this wide phase interval of minimum intensity could be explained with an eccentric orbit and a lower wind density at apastron.

Given our knowledge of both a spin period and an orbital period we can locate the source on the Corbet diagram (Corbet 1986) together with the known P_{spin} and P_{orb} of other binary systems (Bildsten et al. 1997; Liu et al. 2006). We also plot in the diagram the position of the two SFXTs IGR J18483-0311 (Levine & Corbet 2006; Zurita Heras & Chaty 2009) and IGR J11215-5952 (Swank et al. 2007; Sidoli et al. 2007; Romano et al. 2009). IGR J16465–4507 sits at the boundary of the wind-fed OB-HMXBs (systems with OB supergiants that underfill their Roche-lobes) and the locus of the Be transients (Fig. 5).

The characteristics of the system (Lutovinov et al. 2004, 2005) suggested a classification of this source as a SFXT (Negueruela et al. 2006). However, the outburst history of this source is rather scarce. After the initial discovery by *INTEGRAL* no further outbursts have been reported. Walter & Zurita Heras (2007) mention three episodes of enhanced hard X-ray activity observed by *INTEGRAL* at the limit of the instrumental sensitivity, that cannot be considered as real flares. The BAT 15–50 keV light curve during the 54 months of monitoring indicates that this is a faint persistent source, with an average luminosity of 2.6×10^{35} erg s⁻¹ (at a distance of 9.5 kpc), no evidence for flaring activity and a weak variability with a dynamical range lower than 10. Based on their X-ray variability, sgHMXB can be classified as classical and absorbed systems (variability factor < 20) or as SFXT (variability factor > 100). The timing behavior of IGR J16465–4507 suggests a wind-fed system, with a neutron star continuously accreting from a rather homogeneous wind. The luminosity, lower than what observed in classical sgHMXB ($10^{36} - 10^{37}$ erg s⁻¹), can be explained with the larger orbital separation ($\sim 5 R_\star$ compared to $\sim 2 R_\star$ in classical systems).

ACKNOWLEDGMENTS

We thank the anonymous referee for suggestions that helped improve the paper. This work was supported by contracts ASI I/011/07/0 and I/088/06/0.

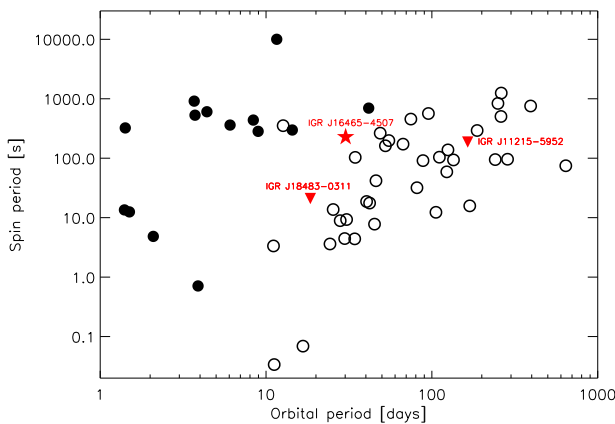


Figure 5. The Corbet diagram showing the neutron star P_{spin} vs. binary period P_{orb} . Black circles are HMXBs with an OB primary, empty circles those with a Be one. Larger (red) symbols represent SFXTs: triangles are IGR J18483–0311 and IGR J11215–5952, the star the newly determined position of IGR J16465–4507.

REFERENCES

Barthelmy S. D., Barbier L. M., Cummings J. R., et al., 2005, *Space Science Reviews*, 120, 143

Bildsten L., Chakrabarty D., Chiu J., et al., 1997, *ApJS*, 113, 367

Bozzo E., Stella L., Israel G., Falanga M., Campana S., 2008, *MNRAS*, 391, L108

Corbet R. H. D., 1986, *MNRAS*, 220, 1047

Cusumano G., La Parola, V., Segreto, A., et al., 2009, *A&A*, 510, 48

Gehrels N., Chincarini G., Giommi P., et al., 2004, *ApJ*, 611, 1005

in't Zand J. J. M., 2005, *A&A*, 441, L1

Jain C., Paul B., Dutta A., 2009, *MNRAS*, 397, L11

Levine A. M., Corbet R., 2006, *Astron. Tel.*, 940, 1

Liu Q. Z., van Paradijs J., van den Heuvel E. P. J., 2006, *A&A*, 455, 1165

Lutovinov A., Revnivtsev M., Gilfanov M., Shtykovskiy P., Molkov S., Sunyaev R., 2005, *A&A*, 444, 821

Lutovinov A., Rodrigues J., Budtz-Jorgensen C., Grebenev S., Winkler C., 2004, *Astron. Tel.*, 329, 1

Martins F., Schaerer D., Hillier D. J., 2005, *A&A*, 436, 1049

Negueruela I., Smith D. M., Reig P., Chaty S., Torrejón J. M., 2006, *ESASP*, 604, 165

Negueruela I., Smith D. M., Harrison T. E., Torrejón J. M., 2006, *ApJ*, 638, 982

Negueruela I., Smith D. M., Torrejón J. M., Reig P., 2007, *ESA Special Publication*, 622, 255

Nespoli E., Fabregat J., Mennickent R. E., 2008, *A&A*, 486, 911

Romano P., Sidoli L., Cusumano G., et al., 2009, *MNRAS*, 399, 2021

Romano P., Sidoli L., Cusumano G., Vercellone S., Mangano V., Krimm H. A., 2009, *ApJ*, 696, 2068

Searle S. C., Prinja R. K., Massa D., Ryans R., 2008, *A&A*, 481, 777

Segreto A., Cusumano G., Ferrigno C., La Parola V., Mangano V., Mineo T., Romano P., 2010, *A&A*, 510, A47

Sguera V., Barlow E. J., Bird A. J., et al., 2005, *A&A*, 444, 221

Sidoli L., Romano, P., Ducci, L., et al. 2009, *MNRAS*, 397, 1528

Sidoli L., Romano P., Mereghetti S., Paizis A., Vercellone S., Mangano V., Götz D., 2007, *A&A*, 476, 1307

Smith D. M., 2004, *ATel*, 338, 1

Swank J. H., Smith D. M., Markwardt C. B., 2007, *Astron. Tel.*, 999, 1

van Paradijs J., 1995, in M. A. Alpar, U. Kiziloglu, & J. van Paradijs ed., *The Lives of the Neutron Stars X-ray Binaries*. pp 281

Walter R., Zurita Heras J., 2007, *A&A*, 476, 335

Zurita Heras J. A., Chaty S., 2009, *A&A*, 493, L1

Zurita Heras J. A., Walter R., 2004, *Astron. Tel.*, 336, 1

This paper has been typeset from a *TeX*/ *L^AT_EX* file prepared by the author.